

The Far-Infrared Laser Magnetic Resonance Spectrum of the CH Radical and Determination of Ground-State Parameters¹

JOHN M. BROWN

Department of Chemistry, Southampton University, Southampton SO9 5NH, England

AND

KENNETH M. EVENSON

National Bureau of Standards, Boulder, Colorado 80303

The far-infrared laser magnetic resonance (LMR) spectrum of the CH radical in the $v = 0$ level of the $X^2\Pi$ state was studied in detail. Nine transitions that are accessible with currently available laser lines were recorded. The measurements were analyzed and subjected to a single least-squares fit using an effective Hamiltonian. The data provide primary information on the rotational and fine-structure intervals between the lowest rotational levels. They also yield values for the Λ -type doubling and proton hyperfine splittings in the same levels.

1. INTRODUCTION

Precise information on the energy levels of the CH radical in its ground $^2\Pi$ state has been particularly hard to come by in the laboratory. For many years, the best available measurements were those obtained in studies of the electronic spectrum (1-3). It was one of the triumphs of the far-infrared laser magnetic resonance (LMR) technique that it was able to achieve the first laboratory detection of transitions within the ground state (4). Equally, it was a notable achievement for the radioastronomers that they were able to observe the three components of the Λ -doubling transition in the lowest rotational level of CH in the interstellar gas clouds (5, 6). The direct detection of these transitions by conventional microwave techniques in the laboratory has yet to be accomplished.

The original observations of the LMR spectrum of the CH radical were made with a water vapor discharge laser at 118.6 μm . The subsequent development of the optically pumped laser system provided a much better frequency coverage of the far-infrared region and enabled Hougen *et al.* (7) to extend the earlier study of CH. Although this work was very thorough and included a complete analysis of the spectra obtained, it cannot be considered definitive for two reasons. First, only three rotational (or spin-rotational) transitions in the ground state of CH were studied; this represents about a third of those that are accessible with currently available laser lines (8). Second, the data relating to the three individual transitions were fitted separately by Hougen *et al.* It has been shown in a companion study of the OH radical (9) that a single

¹ Work supported in part by NASA contract W-15,047.

$^2\Pi$ model Hamiltonian is quite capable of describing all the observable features of the LMR spectrum. The purpose of the present paper is to make good these deficiencies and thereby to derive a set of molecular parameters for CH in its ground state that is as nearly complete as possible. The work is restricted to a consideration of CH in the $v = 0$ level. Spectra for higher vibrational levels and for isotopic modifications (CD, ^{13}CH) have yet to be recorded.

2. EXPERIMENTAL DETAILS

The spectra were recorded at the Boulder laboratories of the NBS with a new far-infrared LMR spectrometer that has been described in detail elsewhere (10). The CH radicals were produced in the spectrometer sample volume by the reaction of fluorine atoms with methane in a flow system, the fluorine atoms being generated by passing a mixture of He and F_2 through a microwave discharge (7). The total pressure in the sample region was about 250 mTorr (33 Pa) which permitted Lamb dips to be observed on all the strong lines. The magnet of the LMR spectrometer was controlled by a rotating coil system which provided a direct readout of the flux densities. The system was calibrated periodically with a proton NMR gaussmeter up to 1.8 T; the overall uncertainty was 10^{-5} T below 0.1 T with a fractional uncertainty of 10^{-4} above 0.1 T (1 tesla = 10^4 gauss).

The far-infrared LMR spectrum of the CH radical in the $v = 0$ level of the $X^2\Pi$ state is summarized in Table I; this includes the observations made in previous studies (4, 7). Nine rotational transitions in CH have been observed using 13 laser lines, as shown in the energy level diagram of Fig. 1. The signal-to-noise ratios were extremely good, equal to about 5000:1 at 1 Hz for the strongest lines. As an example, the low-field portion of the spectrum recorded with the 124.4- μm laser line, arising from the transition $N = 3 \leftarrow 2, J = 2 \ 1/2 \leftarrow 2 \ 1/2$ is shown in Fig. 2. Many additional weak lines were observed that could be assigned to other species present as "impurities." These include OH in vibrational levels $v = 0, 1,$ and 2 (9), NH (11), NH_2 (12), and CH_2 (10). No spectra were observed with the laser lines in Table I that could be attributed to vibrationally excited CH apart from those already reported in the long wavelength spectra around 560 μm (7). It turns out that all the other transitions shown in Fig. 1 depend directly on the rotational constant B . This parameter changes markedly on vibrational excitation (2) and the transition frequencies are shifted out of near coincidence with the corresponding laser frequencies.

When most of the work was completed, we calculated the resonant fields for the most favorable magnetic dipole transitions in CH. We succeeded in observing one such transition, at 659.10 mT in the 124.4- μm σ spectrum. The signal-to-noise ratio was 3:1 with a 1-sec output time constant.

3. ASSIGNMENT AND FITTING

The LMR spectra of the CH radical were assigned with the help of a predictive computer program that has been described earlier (9). The rotational quantum numbers could be assigned simply by a comparison of the molecular transition frequency (2) with the laser frequency. Given reasonable estimates of smaller molecular parameters, it was possible to match the predictions of the computer program (which cal-

TABLE I

Summary of Observations in the Far-Infrared LMR Spectrum of the CH Radical in Its Ground State

Pump	Laser line			CH Transition		
	Gain medium	$\lambda/\mu\text{m}$	ν/GHz	N	J	F_i
9P(34)	CH ₃ OH	70.5	4251.6740(21) ^{a,b}	5 + 4	4 $\frac{1}{2}$ + 3 $\frac{1}{2}$ 5 $\frac{1}{2}$ + 4 $\frac{1}{2}$	$F_2 + F_2$ $F_1 + F_1$
10R(16)	¹³ CH ₃ OH	115.8	2588.3617(13) ^c	3 + 2	2 $\frac{1}{2}$ + 1 $\frac{1}{2}$	$F_2 + F_2$
9R(20)	CH ₂ F ₂	117.7	2546.4950(13) ^d	} 3 + 2	3 $\frac{1}{2}$ + 2 $\frac{1}{2}$	$F_1 + F_1$
Discharge	H ₂ O	118.6	2527.9520(10) ^e			
9P(36)	CH ₃ OH	118.8	2522.7816(13) ^b			
10P(34)	CH ₂ DOH	124.4	2409.2933(12) ^f	3 + 2	2 $\frac{1}{2}$ + 2 $\frac{1}{2}$	$F_2 + F_1$
9P(22)	¹³ CH ₃ OH	149.3	2008.3601(10) ^c	2 + 1	1 $\frac{1}{2}$ + $\frac{1}{2}$	$F_2 + F_2$
10R(34)	CD ₃ OH	180.7	1658.6899(8) ^g	2 + 1	2 $\frac{1}{2}$ + 1 $\frac{1}{2}$	$F_1 + F_1$
10R(16)	¹³ CH ₃ OH	203.6	1472.1993(7) ^c	2 + 1	1 $\frac{1}{2}$ + 1 $\frac{1}{2}$	$F_2 + F_1$
10P(14)	CH ₂ CF ₂	554.4	540.7851(20) ^h	} 1 + 1	1 $\frac{1}{2}$ + $\frac{1}{2}$	$F_1 + F_2$
10P(20)	DCOOD	561.3	534.1096(5) ⁱ			
10P(16)	CH ₂ CHCl	567.9	527.8539(10) ^h			
9P(16)	CH ₃ OH	570.6	525.4275(3) ^b			

^a The figures in parentheses give the uncertainty in the laser frequency, in units of the last quoted decimal place.

^b F.R. Petersen, K.M. Evenson, D.A. Jennings and A. Scalabrin, *IEEE J. Quant. Electron.* QE-16, 319-323 (1980).

^c J.O. Henningsen, J.C. Petersen, F.R. Petersen, D.A. Jennings and K.M. Evenson, *J. Mol. Spectrosc.* 77, 298-309 (1979).

^d F.R. Petersen, A. Scalabrin and K.M. Evenson, *Int. J. IR & mm Waves*, 1, 111-115 (1980).

^e F.R. Petersen, K.M. Evenson, D.A. Jennings, J.S. Wells, K. Goto and J.J. Jimenez, *IEEE J. Quant. Electron.* QE-11, 838-843 (1976).

^f A. Scalabrin, F.R. Petersen, K.M. Evenson and D.A. Jennings, *Int. J. IR & mm Waves*, 1, 117-125 (1980).

^g K.M. Evenson, F.R. Petersen and D.A. Jennings, to be published.

^h H.E. Radford, F.R. Petersen, D.A. Jennings and J.A. Mucha, *IEEE J. Quant. Electron.* QE-13, 92-94 (1977).

ⁱ S.F. Dyubko, V.A. Svich and L.D. Fese ko, *Sov. Phys. Tech. Phys.* 20, 1536-1538 (1976).

culates all possible Zeeman transitions above a selected intensity) with the experimental spectra and thus to make the assignments directly. The full details of the experimental measurements and their assignments are given in Table II. For the most part, the transitions obey the expected selection rule $\Delta M_J = 0$ (π polarization) or ± 1 (σ) and $\Delta M_I = 0$. In addition, a number of weaker transitions which are formally forbidden ($\Delta M_I = \pm 1$) are also observed. For the 124.4- and 203.6- μm spectra, this

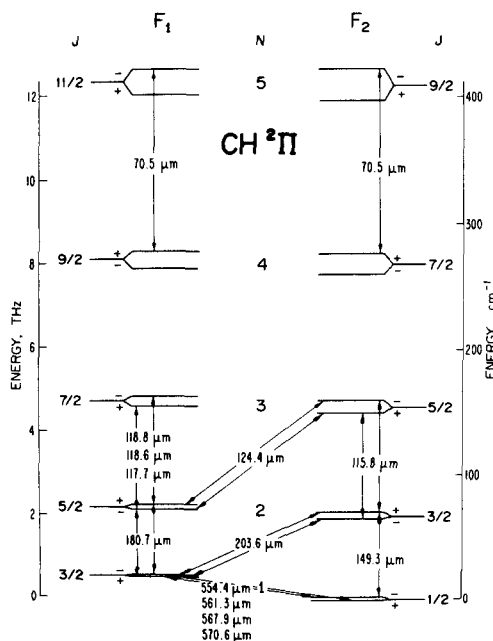


FIG. 1. Diagram showing the lower energy levels of CH in the $X^2\Pi$ state and the transitions involved in the observed far-infrared LMR spectrum. The Λ -type (parity) doubling has been exaggerated by a factor of 20 for clarity.

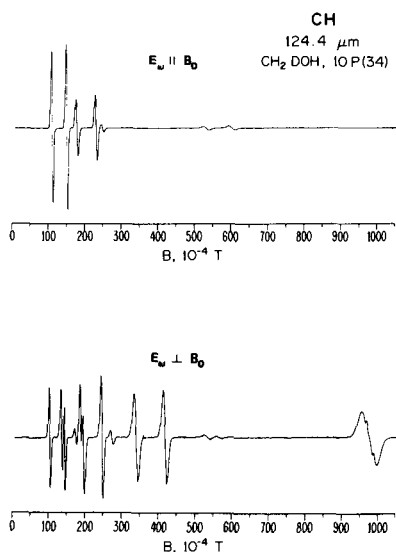


FIG. 2. The low-field portion of the 124.4- μm LMR spectrum of the CH radical, in parallel (π) and perpendicular (σ) polarization. The rotational transition involved is $N = 3 \leftarrow 2$, $J = 2 \ 1/2 \leftarrow 2 \ 1/2$. Some of the weaker lines arise from nuclear spin "forbidden" transitions with $\Delta M_I \neq 0$ (see Table II). Note the Lamp dips on the line at the high-field end of the σ spectrum.

TABLE II

Flux Densities and Frequencies of Transitions Observed by LMR for CH in the $X^2\Pi$ State

Parity ^a	$M_{J'}$	M_I	$M_{J''}$	M_I	Flux Density (mT)	$\nu_{\text{laser}} - \nu_{\text{calc}}^b$ (MHz)	Weight (MHz ⁻²)
70.5 μm spectrum $F_2, J = 4\frac{1}{2} + F_2, J = 3\frac{1}{2}$ and $F_1, J = 5\frac{1}{2} + F_1, J = 4\frac{1}{2}$ (High field doublet)							
-polarisation (π) No transitions observed below 2.2 Tesla.							
⊥ -polarisation (σ)							
+	$1\frac{1}{2}$	$-\frac{1}{2}$	$2\frac{1}{2}$	$-\frac{1}{2}$	787.10	-2.1	0.1106
+	$1\frac{1}{2}$	$-\frac{1}{2}$	$2\frac{1}{2}$	$-\frac{1}{2}$	812.30*	-5.9	0.1106
+	$\frac{1}{2}$	$-\frac{1}{2}$	$1\frac{1}{2}$	$-\frac{1}{2}$	844.72*	8.8	0.1106
+	$\frac{1}{2}$	$-\frac{1}{2}$	$1\frac{1}{2}$	$-\frac{1}{2}$	867.88*	5.8	0.1106
+	$-\frac{1}{2}$	$-\frac{1}{2}$	$\frac{1}{2}$	$-\frac{1}{2}$	926.56*	16.3	0.1106
+	$-\frac{1}{2}$	$-\frac{1}{2}$	$\frac{1}{2}$	$-\frac{1}{2}$	948.65*	13.6	0.1106
+	$-1\frac{1}{2}$	$-\frac{1}{2}$	$-\frac{1}{2}$	$-\frac{1}{2}$	1044.36*	25.2	0.1106
+	$-1\frac{1}{2}$	$-\frac{1}{2}$	$-\frac{1}{2}$	$-\frac{1}{2}$	1067.32*	22.8	0.1106
+	$-1\frac{1}{2}$	$-\frac{1}{2}$	$-\frac{1}{2}$	$-\frac{1}{2}$	1818.29*	78.8	0.0
+	$-1\frac{1}{2}$	$-\frac{1}{2}$	$-\frac{1}{2}$	$-\frac{1}{2}$	1841.60*	85.7	0.0
+	$-3\frac{1}{2}$	$-\frac{1}{2}$	$-4\frac{1}{2}$	$-\frac{1}{2}$	1948.77	-54.3	0.0
+	$-3\frac{1}{2}$	$-\frac{1}{2}$	$-4\frac{1}{2}$	$-\frac{1}{2}$	1950.73	-54.6	0.0
115.8 μm spectrum $F_2, J = 2\frac{1}{2} + F_2, J = 1\frac{1}{2}$							
- polarisation (π)							
+	$1\frac{1}{2}$	$\frac{1}{2}$	$1\frac{1}{2}$	$\frac{1}{2}$	1770.74*	-6.3	0.2985
+	$1\frac{1}{2}$	$-\frac{1}{2}$	$1\frac{1}{2}$	$-\frac{1}{2}$	1776.82*	-6.5	0.2985
⊥ -polarisation (σ)							
-	$-2\frac{1}{2}$	$\frac{1}{2}$	$-1\frac{1}{2}$	$\frac{1}{2}$	654.90*	-5.0	0.2985
-	$-2\frac{1}{2}$	$-\frac{1}{2}$	$-1\frac{1}{2}$	$-\frac{1}{2}$	655.37*	-5.0	0.2985
-	$-1\frac{1}{2}$	$-\frac{1}{2}$	$-3\frac{1}{2}$	$-\frac{1}{2}$	1118.18*	-5.2	0.2985
-	$-1\frac{1}{2}$	$\frac{1}{2}$	$-1\frac{1}{2}$	$\frac{1}{2}$	1122.80*	-5.2	0.2985
+	$2\frac{1}{2}$	$\frac{1}{2}$	$1\frac{1}{2}$	$\frac{1}{2}$	1207.11*	-5.1	0.2985
+	$2\frac{1}{2}$	$1\frac{1}{2}$	$1\frac{1}{2}$	$-\frac{1}{2}$	1207.60*	-5.1	0.2985
+	$1\frac{1}{2}$	$-\frac{1}{2}$	$\frac{1}{2}$	$-\frac{1}{2}$	1592.25*	-5.1	0.2985
+	$1\frac{1}{2}$	$\frac{1}{2}$	$\frac{1}{2}$	$-\frac{1}{2}$	1595.88*	-5.5	0.2985
+	$\frac{1}{2}$	$-\frac{1}{2}$	$-\frac{1}{2}$	$-\frac{1}{2}$	2048.1*	1.1	0.0
+	$\frac{1}{2}$	$\frac{1}{2}$	$-\frac{1}{2}$	$\frac{1}{2}$	2057.7	0.4	0.0
117.7 μm spectrum $F_1, J = 3\frac{1}{2} + F_1, J = 2\frac{1}{2}$							
⊥ - polarisation							
+	$-1\frac{1}{2}$	$-\frac{1}{2}$	$-2\frac{1}{2}$	$-\frac{1}{2}$	1231.95	-3.1	0.0
+	$-1\frac{1}{2}$	$-\frac{1}{2}$	$-2\frac{1}{2}$	$-\frac{1}{2}$	1233.32*	-3.8	0.0
+	$-\frac{1}{2}$	$-\frac{1}{2}$	$-1\frac{1}{2}$	$-\frac{1}{2}$	1557.58*	-3.6	0.0
+	$-\frac{1}{2}$	$\frac{1}{2}$	$-1\frac{1}{2}$	$\frac{1}{2}$	1558.94*	-3.7	0.0
-	$-1\frac{1}{2}$	$-\frac{1}{2}$	$-2\frac{1}{2}$	$-\frac{1}{2}$	1685.00	-0.6	0.0
-	$-1\frac{1}{2}$	$\frac{1}{2}$	$-2\frac{1}{2}$	$\frac{1}{2}$	1685.92	-1.7	0.0

is due to some resonances at very low fields where the proton spin is not completely decoupled from the rotational angular momentum J . Some of these lines can be seen in Fig. 2. The "forbidden" transitions are also detected in the 149.3- μm spectrum, this time at high flux densities. The reason for this observation is that the lower level for this transition is $J = 1/2$ which has essentially pure $\Omega = 1/2$ character. Consequently the orbital and spin contributions to the magnetic moment largely cancel out and the Zeeman effect depends on the smaller g factors. The residual electron orbital and spin magnetic moment is almost exactly canceled by the proton nuclear

TABLE II—Continued

Parity ^a	M_J'	M_I'	M_J	M_I	Flux Density (mT)	$\nu_{\text{laser}} - \nu_{\text{calc}}^b$ (MHz)	Weight (MHz ⁻²)
124.4 μm spectrum $F_2, J = 2\frac{1}{2} + F_1, J = 2\frac{1}{2}$							
-polarisation (π)							
+	$2\frac{1}{2}$	$-\frac{1}{2}$	$2\frac{1}{2}$	$-\frac{1}{2}$	9.05*	-3.6	0.3446
+	$1\frac{1}{2}$	$\frac{1}{2}$	$2\frac{1}{2}$	$-\frac{1}{2}$	13.05*	-3.6	0.3446
+	$2\frac{1}{2}$	$\frac{1}{2}$	$2\frac{1}{2}$	$\frac{1}{2}$	13.05*	-0.1	0.0
+	$1\frac{1}{2}$	$-\frac{1}{2}$	$1\frac{1}{2}$	$-\frac{1}{2}$	15.81*	-3.8	0.3446
+	$1\frac{1}{2}$	$\frac{1}{2}$	$1\frac{1}{2}$	$\frac{1}{2}$	21.05	-3.6	0.3446
+	$\frac{1}{2}$	$\frac{1}{2}$	$1\frac{1}{2}$	$-\frac{1}{2}$	22.86	-3.0	0.3446
+	$\frac{1}{2}$	$-\frac{1}{2}$	$\frac{1}{2}$	$-\frac{1}{2}$	51.24	-2.8	0.3446
+	$\frac{1}{2}$	$\frac{1}{2}$	$\frac{1}{2}$	$\frac{1}{2}$	58.20	-2.9	0.3446
-	$-2\frac{1}{2}$	$-\frac{1}{2}$	$-2\frac{1}{2}$	$-\frac{1}{2}$	431.61*	0.0	0.3446
-	$-2\frac{1}{2}$	$\frac{1}{2}$	$-2\frac{1}{2}$	$\frac{1}{2}$	433.51*	0.1	0.3446
-	$-1\frac{1}{2}$	$-\frac{1}{2}$	$-1\frac{1}{2}$	$-\frac{1}{2}$	793.96*	0.9	0.3446
-	$-1\frac{1}{2}$	$\frac{1}{2}$	$-1\frac{1}{2}$	$\frac{1}{2}$	795.75*	0.6	0.3446
⊥-polarisation (σ)							
+	$1\frac{1}{2}$	$-\frac{1}{2}$	$2\frac{1}{2}$	$-\frac{1}{2}$	10.21	-2.2	0.3446
+	$2\frac{1}{2}$	$-\frac{1}{2}$	$1\frac{1}{2}$	$-\frac{1}{2}$	13.44	-2.9	0.3446
+	$\frac{1}{2}$	$\frac{1}{2}$	$2\frac{1}{2}$	$-\frac{1}{2}$	14.25	-1.6	0.0
+	$1\frac{1}{2}$	$\frac{1}{2}$	$2\frac{1}{2}$	$\frac{1}{2}$	14.25	-3.1	0.3446
+	$2\frac{1}{2}$	$\frac{1}{2}$	$1\frac{1}{2}$	$\frac{1}{2}$	18.55	-3.2	0.3446
+	$\frac{1}{2}$	$-\frac{1}{2}$	$1\frac{1}{2}$	$-\frac{1}{2}$	19.39	-2.8	0.3446
+	$\frac{1}{2}$	$\frac{1}{2}$	$1\frac{1}{2}$	$\frac{1}{2}$	24.43	-3.1	0.3446
+	$-\frac{1}{2}$	$-\frac{1}{2}$	$1\frac{1}{2}$	$-\frac{1}{2}$	27.15*	-3.2	0.3446
+	$1\frac{1}{2}$	$-\frac{1}{2}$	$\frac{1}{2}$	$-\frac{1}{2}$	33.67*	-3.2	0.3446
+	$1\frac{1}{2}$	$\frac{1}{2}$	$\frac{1}{2}$	$\frac{1}{2}$	41.58	-3.3	0.3446
+	$\frac{1}{2}$	$-\frac{1}{2}$	$\frac{1}{2}$	$\frac{1}{2}$	53.09*	-3.1	0.3446
+	$-\frac{1}{2}$	$-\frac{1}{2}$	$\frac{1}{2}$	$-\frac{1}{2}$	96.24*	-3.3	0.3446
+	$-\frac{1}{2}$	$\frac{1}{2}$	$\frac{1}{2}$	$-\frac{1}{2}$	98.34*	-3.2	0.3446
-	$-1\frac{1}{2}$	$-\frac{1}{2}$	$-2\frac{1}{2}$	$-\frac{1}{2}$	482.30	-0.7	0.3446
-	$-1\frac{1}{2}$	$\frac{1}{2}$	$-2\frac{1}{2}$	$\frac{1}{2}$	483.63	-0.8	0.3446
-	$-2\frac{1}{2}$	$-\frac{1}{2}$	$-1\frac{1}{2}$	$-\frac{1}{2}$	652.07	-0.6	0.3446
-	$-2\frac{1}{2}$	$\frac{1}{2}$	$-1\frac{1}{2}$	$\frac{1}{2}$	654.67*	-0.6	0.3446
-	$-\frac{1}{2}$	$-\frac{1}{2}$	$-1\frac{1}{2}$	$-\frac{1}{2}$	1017.94*	0.2	0.3446
-	$-\frac{1}{2}$	$\frac{1}{2}$	$-1\frac{1}{2}$	$\frac{1}{2}$	1018.19*	0.0	0.3446
+	$\frac{1}{2}$	$-\frac{1}{2}$	$-\frac{1}{2}$	$-\frac{1}{2}$	1187.97*	-3.4	0.3446
+	$\frac{1}{2}$	$\frac{1}{2}$	$-\frac{1}{2}$	$\frac{1}{2}$	1193.26*	-3.4	0.3446
+	$-2\frac{1}{2}$	$\frac{1}{2}$	$-2\frac{1}{2}$	$\frac{1}{2}$	659.10 ^c	7.3	0.2066
149.3 μm spectrum $F_2, J = 1\frac{1}{2} + F_2, J = \frac{1}{2}$							
-polarisation (π)							
-	$\frac{1}{2}$	$-\frac{1}{2}$	$\frac{1}{2}$	$-\frac{1}{2}$	1633.83*	3.5	0.4958
-	$\frac{1}{2}$	$\frac{1}{2}$	$\frac{1}{2}$	$\frac{1}{2}$	1635.32*	4.2	0.4958
-	$\frac{1}{2}$	$-\frac{1}{2}$	$-\frac{1}{2}$	$\frac{1}{2}$	1672.65*	0.3	0.4958
⊥-polarisation (σ)							
-	$1\frac{1}{2}$	$-\frac{1}{2}$	$\frac{1}{2}$	$-\frac{1}{2}$	1348.80*	4.3	0.4958
-	$1\frac{1}{2}$	$\frac{1}{2}$	$\frac{1}{2}$	$\frac{1}{2}$	1367.18*	4.5	0.4958
-	$1\frac{1}{2}$	$-\frac{1}{2}$	$-\frac{1}{2}$	$\frac{1}{2}$	1388.69*	2.0	0.4958
-	$\frac{1}{2}$	$\frac{1}{2}$	$-\frac{1}{2}$	$-\frac{1}{2}$	1616.12*	3.9	0.4958
-	$\frac{1}{2}$	$-\frac{1}{2}$	$-\frac{1}{2}$	$\frac{1}{2}$	1623.81*	0.2	0.4958
-	$\frac{1}{2}$	$\frac{1}{2}$	$-\frac{1}{2}$	$\frac{1}{2}$	1654.34*	0.9	0.4958

magnetic moment and the nuclear spin remains coupled even for large flux densities. Similar effects have been observed in the LMR spectrum of the OH radical (9). The transitions in CH for which Lamb dips were observed are marked in Table II with an asterisk.

TABLE II—Continued

Parity ^a	M_J'	M_I'	M_J	M_I	Flux Density (mT)	ν_{laser} ^c ν_{calc} ^b (MHz)	Weight (MHz ⁻²)
203.6 μm spectrum $F_2, J = 1\frac{1}{2} + F_1, J = 1\frac{1}{2}$							
-polarisation (π)							
+	$-1\frac{1}{2}$	$-\frac{1}{2}$	$-1\frac{1}{2}$	$-\frac{1}{2}$	75.21	2.5	0.5000
+	$-1\frac{1}{2}$	$\frac{1}{2}$	$-1\frac{1}{2}$	$\frac{1}{2}$	76.53	2.3	0.5000
+	$-\frac{1}{2}$	$-\frac{1}{2}$	$-1\frac{1}{2}$	$-\frac{1}{2}$	79.63	1.4	0.5000
+	$-\frac{1}{2}$	$\frac{1}{2}$	$-\frac{1}{2}$	$-\frac{1}{2}$	235.49	3.1	0.5000
+	$-\frac{1}{2}$	$\frac{1}{2}$	$-\frac{1}{2}$	$\frac{1}{2}$	236.33	2.5	0.5000
-	$1\frac{1}{2}$	$-\frac{1}{2}$	$1\frac{1}{2}$	$-\frac{1}{2}$	260.58	3.7	0.5000
-	$1\frac{1}{2}$	$\frac{1}{2}$	$1\frac{1}{2}$	$\frac{1}{2}$	264.39	3.7	0.5000
-	$\frac{1}{2}$	$-\frac{1}{2}$	$\frac{1}{2}$	$-\frac{1}{2}$	716.93	2.5	0.5000
-	$\frac{1}{2}$	$\frac{1}{2}$	$\frac{1}{2}$	$\frac{1}{2}$	720.84	2.6	0.5000
-polarisation (σ)							
+	$-1\frac{1}{2}$	$\frac{1}{2}$	$-1\frac{1}{2}$	$-\frac{1}{2}$	76.77	3.1	0.5000
+	$-1\frac{1}{2}$	$\frac{1}{2}$	$-1\frac{1}{2}$	$\frac{1}{2}$	79.38*	3.0	0.5000
+	$-\frac{1}{2}$	$-\frac{1}{2}$	$-1\frac{1}{2}$	$-\frac{1}{2}$	79.80*	3.7	0.5000
+	$-\frac{1}{2}$	$\frac{1}{2}$	$-\frac{1}{2}$	$-\frac{1}{2}$	83.88*	3.1	0.5000
+	$-1\frac{1}{2}$	$-\frac{1}{2}$	$-\frac{1}{2}$	$-\frac{1}{2}$	203.23*	3.8	0.5000
+	$-1\frac{1}{2}$	$\frac{1}{2}$	$-\frac{1}{2}$	$\frac{1}{2}$	207.90*	4.1	0.5000
+	$-\frac{1}{2}$	$-\frac{1}{2}$	$-\frac{1}{2}$	$-\frac{1}{2}$	271.42	3.3	0.5000
-	$\frac{1}{2}$	$-\frac{1}{2}$	$1\frac{1}{2}$	$-\frac{1}{2}$	272.59	1.5	0.5000
-	$\frac{1}{2}$	$\frac{1}{2}$	$1\frac{1}{2}$	$\frac{1}{2}$	274.95	2.2	0.5000
+	$\frac{1}{2}$	$-\frac{1}{2}$	$-\frac{1}{2}$	$-\frac{1}{2}$	275.29*	3.3	0.0
-	$1\frac{1}{2}$	$-\frac{1}{2}$	$\frac{1}{2}$	$-\frac{1}{2}$	655.71*	2.1	0.5000
-	$1\frac{1}{2}$	$\frac{1}{2}$	$\frac{1}{2}$	$\frac{1}{2}$	663.54*	1.9	0.5000
-	$-\frac{1}{2}$	$-\frac{1}{2}$	$\frac{1}{2}$	$\frac{1}{2}$	808.03*	1.6	0.5000
-	$-\frac{1}{2}$	$\frac{1}{2}$	$-\frac{1}{2}$	$-\frac{1}{2}$	809.66	6.4	0.5000

^a Parity of lower state.

^b Calculated frequency obtained using the parameter values from Table II.

^c Magnetic dipole transition.

The data in Table II were used in conjunction with the earlier LMR measurements (7) and the microwave frequencies measured by the radioastronomers (13) to determine an optimal set of molecular parameters for CH in the $v = 0$ level of the $X^2\Pi$ state. The Hamiltonian used was the N^2 version advocated by Brown *et al.* (14) and described in the fit of the OH data (9). The CH molecule in its ground state conforms very closely to the Hund's coupling case (b) limit ($A = 2B$, where A is the spin-orbit coupling constant). The pattern of energy levels is therefore described quite well by the expression $B N(N + 1)$, where N is the rotational quantum number taking values 0, 1, 2, . . . Each such N level is split into a spin-rotation doublet, the two components of which can be distinguished by the value of the quantum number J (see Fig. 1). We have therefore determined combinations of parameters appropriate to the case (b) limit; for example, the Λ -doubling parameters p and q are better determined than case (a) combinations $(p + 2q)$ and q . Since it is not possible to determine both the parameters A_D and γ in a fit of single species in a $^2\Pi$ state, we have performed the fit with the former constrained to zero. Consequently, the parameters determined as A and γ take effective values, denoted by a tilde (e.g., \tilde{A}) in our results. The fit

TABLE III
Parameters for CH in the $v = 0$ Level of the $X^2\Pi$ State^a

\tilde{A}	843818.1(19) ^b	B	425474.97(22)
$\tilde{\gamma}$	-770.88(72)	D	43.700(11)
γ_D	0.135(73)	$10^2 H$	0.350 ^c
P	1005.43(62)	q	1159.01(27)
P_D	-0.445(77)	q_D	-0.393(15)
a	54.7(16)	c	58.2(39)
b_F	-57.5(13)	d	43.480(10)
g_L'	1.00103(12)	$10^2 g_p$	-0.2812(51)
g_S	2.0020 ^c	$10^2 g_k'$	0.1182 ^c
$10^2 g_k$	0.101(19)	$10^2 g_p^{e'}$	-0.2724 ^c

^a Value in MHz, where appropriate.

^b The numbers in parenthesis represent one standard deviation of the least-squares fit, in units of the last quoted decimal place.

^c Parameter constrained to this value in the least-squares fit.

performed with γ constrained to zero is definitely inferior for CH, as we discuss in the next section.

The basis set was truncated without loss in accuracy at $\Delta N = \pm 1$ rather than $\Delta J = \pm 1$, again a reflection of the Hund's case (b) behavior of CH. Each datum was weighted in the fit inversely as the square of the experimental error; the weights are given in Table II. The main contribution to the error comes from the uncertainty in the knowledge of the far-infrared laser frequencies ($\sim 5 \times 10^{-7}$); this information is given in Table I.

The results of the fit are given in Table II and the parameter values determined in the process are given in Table III. The data set was not quite large or precise enough to determine all the parameters and a few had to be constrained to values estimated from other sources. The sextic centrifugal distortion constant H was calculated from the formula

$$H_0 \simeq H_e = 2/3D_e\{12(B_e/\omega_e)^2 - \alpha_e/\omega_e\}, \quad (1)$$

where the subscript e denotes an equilibrium value and ω_e and α_e are the harmonic vibrational frequency and the anharmonic correction to the rotational constant, respectively. Furthermore, it proved possible to determine no more than three of the six g factors required for a molecule in a $^2\Pi$ state. This was not altogether surprising

in view of the lack of more precise information on the Zeeman effect from sources such as the EPR spectrum. We have estimated a value for the electron spin g factor of 2.0020, corresponding to a relativistic correction of 1.5×10^{-4} . The two Λ -doubling g factors g'_l and g'_r were estimated from the relationships

$$g'_l = p/2B, \quad (2)$$

$$g'_r = -q/B, \quad (3)$$

which proved very reliable for OH in its $X^2\Pi$ state (9). The standard deviation of the fit relative to the experimental uncertainty was 2.22, a figure which is adequate rather than completely satisfactory. The residuals in Table II show that the main cause of the poor fit is in the data for the 70.5- μm spectrum. We have not been able to establish the reason for this behavior. It is possible to improve the fit by varying additional parameters such as H but since this causes D to deviate by an unacceptable amount from the expected value (2), we are not convinced that this is the right explanation.

4. DISCUSSION

The present analysis of the far-infrared LMR spectrum of the CH radical has led to a precise determination of its low-lying spin-rotation levels. The parameter set in Table III is consistent with the only previous determination, that by Herzberg and Johns (2) but is considerably more precise and extensive. Their values, for comparison are

$$A_0 = 837.9 \text{ GHz}, \quad B_0 = 425.41 \text{ GHz},$$

$$D_0 = 42.9 \text{ MHz}, \quad q = 900 \text{ MHz}$$

(no error limits are quoted). In addition to the detection of the Λ -doubling transitions of CH in the lowest rotational level by radioastronomers (5, 6), far-infrared transitions in similar molecules like OH have also been observed in astrophysical sources (15). There is thus an interest in the frequencies of all electric-dipole allowed transitions between the lower levels of CH to aid future astronomical searches. We have performed the necessary calculations using the parameters in Table III; the collective results are to be published elsewhere (16).

We have chosen to fit the data for CH with the parameter A_D constrained to zero. In consequence, the values of the parameters obtained, particularly those for \tilde{A} and $\tilde{\gamma}$, are effective values (17)

$$\tilde{A} = A\{1 + A_D/2B\}, \quad (4)$$

$$\tilde{\gamma} = \gamma - A_D(A - 2B)/2B. \quad (5)$$

It can be seen that for CH, with $A \simeq 2B$, the value determined for $\tilde{\gamma}$ depends only very slightly on the parameter A_D . This will not be the case for CD so that it should be possible to separate γ and A_D once the value of $\tilde{\gamma}$ for CD has been determined. We have also fit the same data set with γ rather than A_D constrained to zero but have found this to be much inferior. The fit converged very slowly, the ultimate standard deviation of fit was larger and the parameters were more highly correlated.

The reduction of the Hamiltonian chosen in this case is simply not appropriate. For example, the effective parameter \tilde{A}_D is given by

$$\tilde{A}_D = A_D - 2B\gamma/(A - 2B), \quad (6)$$

a quantity which becomes indeterminate when $A = 2B$. The same type of behavior has been observed in the description of centrifugal distortion of rotational energy of near-symmetric top molecules with a Hamiltonian that is appropriate for a fully asymmetric top instead (18).

Four Λ -doubling parameters have been determined in the fit (p , p_D , q , and q_D), anchored by the very precise astrophysical measurements (13). The value for p does not agree very well with $-2\tilde{\gamma}$, the value it would be expected to take if the ${}^2\Pi$ state were perturbed only by ${}^2\Sigma^+$ states (14). This probably implies that the $X^2\Pi$ state is contaminated to some extent by ${}^2\Delta$ states. Alternatively, there may be significant spin-orbit coupling with the low-lying $a^4\Sigma^-$ state (19) although the indications are that in this case the relationship $p = -2\gamma$ is maintained. The sign of the parameter q , on the other hand, shows that the effects of perturbation by ${}^2\Sigma^-$ states outweigh those from ${}^2\Sigma^+$ states. Consideration of these two parameters alone therefore shows that the levels of the $X^2\Pi$ state of CH would not be well described by a unique perturber model (20), in contrast to the corresponding state of OH. This conclusion is not very surprising since the first excited configuration of CH ($1\sigma^2 2\sigma^2 3\sigma^1 \pi^2$) gives rise to several electronic states (${}^4\Sigma^-$, ${}^2\Delta$, ${}^2\Sigma^-$, and ${}^2\Sigma^+$), all of which can be mixed to differing degrees with the ground ${}^2\Pi$ state. The values determined by the centrifugal correction parameters p_D and q_D do not agree well with the estimates based on formulae due to Veseth (21):

$$p_D = -2pD/B, \quad q_D = -4qD/B. \quad (7)$$

The estimates are -0.207 and -0.476 MHz, respectively, to be compared with the experimental values of $-0.445(77)$ and $-0.393(15)$.

All four proton hyperfine parameters have been determined in our fit. Previously only one had been determined experimentally, namely d , which is precisely defined by the astrophysical data. However, Levy and Hinze (22) have calculated values for the three other parameters *ab initio*. Their values for the Frosch and Foley combinations a , b ($=b_F - 1/3c$), and c are 58.5 ± 4.5 , -72 ± 10 , and 57 ± 4 MHz which compare well with our values (54.7 ± 1.6 , -76.9 ± 1.8 , and 58.2 ± 3.9 , respectively). A good first-order description of the electronic wavefunction for CH in its ground state places the unpaired electron in a $2p\pi$ orbital on the carbon atom. The value for the Fermi contact parameter b_F in Table III is negative as expected since this contribution to the interaction at the proton arises by spin polarization. Indeed the CH molecule is really the prototype fragment for the application of McConnell's relationship that has been used to estimate the distribution of electron spin densities in aromatic hydrocarbon radicals (23, 24). On this basis, the spin density at the C nucleus is calculated to be 0.91, close to the value of unity that is expected. As an aside, we note that the value determined for the spin-orbit coupling parameter A is also consistent with the unpaired electron spin density being confined to the C atom (the value for the spin-orbit coupling constant ζ for a single electron in a carbon $2p$

orbital is 27.5 cm^{-1} (25)). If the orbital and spin angular momenta are carried by the same electron, the relationship

$$c = 3(a - d) \quad (8)$$

is valid. Using the values given in Table III, the quantity on the right-hand side is calculated to be 33.7 MHz (cf., $c = 55.9 \text{ MHz}$). A similarly poor agreement was found by Radford for OH (26).

Finally, we have determined values for three of the six possible g factors for a molecule in a ${}^2\Pi$ state. The orbital g factor g_L' deviates from unity because of relativistic and nonadiabatic corrections. The former is typically about -1.5×10^{-4} , from which the nonadiabatic correction, Δg_L , is calculated to be $1.16(13) \times 10^{-2}$. The rotational g factor g_r has nuclear and electronic contributions:

$$g_r = g_r^N - g_r^e. \quad (9)$$

The nuclear contribution depends only on the nuclear masses and charges for a diatomic molecule; for CH, it is calculated to be 5.249×10^{-4} (in units of Bohr magnetons) leaving g_r^e as $0.3358(55) \times 10^{-2}$. The two parameters Δg_L and g_r^e have essentially the same physical origin in the effective Hamiltonian, both depending on the admixture of ${}^2\Sigma$ and ${}^2\Delta$ states (27). However, while Δg_L depends on the difference of these two effects, g_r^e depends on their sum. Thus if a ${}^2\Pi$ state is contaminated by ${}^2\Sigma$ states alone, Δg_L is equal to g_r^e . Our experimental results show clearly that this is not the case and we thus have further evidence that both ${}^2\Sigma$ and ${}^2\Delta$ states are mixed into the $X^2\Pi$ state of CH. The third g factor determined in our fit is the anisotropic correction to the electron spin magnetic moment, g_l . The value in Table III (0.96×10^{-3}) does not agree very well with the expectations of Curl's relationship (28), $-\gamma/2B$ or 0.69×10^{-3} . It is possible that this is caused by perturbations with the nearby $a^4\Sigma^-$ state of CH.

It can be seen from this work that the detailed study of the far-infrared spectrum of even a simple molecule like CH can be very rewarding. However, much still remains to be done. We are currently making a similar study of CD. In addition to being of interest in its own right, the study of this species also permits a deeper understanding of its properties when combined with the results for CH. Similarly, a study of ${}^{13}\text{CH}$ would be worthwhile, particularly for more information on the electronic wavefunction from the hyperfine interactions. The signal-to-noise ratios of lines for the parent molecule suggest that it should be possible to detect this isotopic variant in natural abundance (1.1%). The $\text{F} + \text{CH}_4$ reaction used to generate CH radicals in this work liberates a lot of energy in the process. Indeed, in the earlier work on the 550 to 560- μm spectrum (7), it was possible to identify transitions for CH in vibrational levels $v = 1$ and 2. A systematic study of vibrationally excited CH is therefore feasible and would yield much of interest.

RECEIVED: December 9, 1982

REFERENCES

1. L. GERÖ, *Z. Phys.* **118**, 27-36 (1941).
2. G. HERZBERG AND J. W. C. JOHNS, *Astrophys. J.* **158**, 399-418 (1969).

3. A. E. DOUGLAS AND G. A. ELLIOTT, *Can. J. Phys.* **43**, 496-502 (1965).
4. K. M. EVENSON, H. F. RADFORD, AND M. M. MORAN, JR., *Appl. Phys. Lett.* **18**, 426-429 (1971).
5. O. E. H. RYDBECK, J. ELLDÉR, AND W. M. IRVINE, *Nature (London)* **246**, 466-468 (1973).
6. B. E. TURNER AND B. ZUCKERMAN, *Astrophys. J. Lett.* **187**, L59-L62 (1974).
7. J. T. HOUGEN, J. A. MUCHA, D. A. JENNINGS, AND K. M. EVENSON, *J. Mol. Spectrosc.* **72**, 463-483 (1978).
8. D. J. E. KNIGHT, "Ordered List of Far Infrared Laser Lines," NPL Report Qu 45, Feb. 1981.
9. J. M. BROWN, C. M. L. KERR, F. D. WAYNE, K. M. EVENSON, AND H. E. RADFORD, *J. Mol. Spectrosc.* **86**, 544-554 (1981).
10. T. J. SEARS, P. R. BUNKER, A. R. W. MCKELLAR, K. M. EVENSON, D. A. JENNINGS, AND J. M. BROWN, *J. Chem. Phys.* **77**, 5348-5362 (1982).
11. F. D. WAYNE AND H. E. RADFORD, *Mol. Phys.* **32**, 1407-1422 (1976).
12. P. B. DAVIES, D. K. RUSSELL, B. A. THRUSH, AND H. E. RADFORD, *Proc. Roy. Soc. London A* **353**, 299-318 (1977).
13. O. E. H. RYDBECK, J. ELLDÉR, W. M. IRVINE, A. SUME, AND Å HJALMARSON, *Astron. Astrophys.* **34**, 479-482 (1974).
14. J. M. BROWN, E. A. COLBOURN, J. K. G. WATSON, AND F. D. WAYNE, *J. Mol. Spectrosc.* **74**, 294-318 (1979).
15. J. W. V. STOREY, D. M. WATSON, AND C. H. TOWNES, *Astrophys. J. Lett.* **244**, L27-L30 (1980).
16. J. M. BROWN AND K. M. EVENSON, *Astrophys. J.*, in press.
17. J. M. BROWN AND J. K. G. WATSON, *J. Mol. Spectrosc.* **65**, 65-74 (1977).
18. J. K. G. WATSON, in "Vibrational Spectra and Structure" (J. R. Durig, Ed.), Vol. 6, Elsevier, Amsterdam, 1977.
19. A. KASDAN, E. HERBST, AND W. C. LINEBERGER, *Chem. Phys. Lett.* **31**, 78-82 (1975).
20. R. N. ZARE, A. L. SCHMELTEKOPF, W. J. HARROP, AND D. L. ALBRITTON, *J. Mol. Spectrosc.* **46**, 37-66 (1973).
21. L. VESETH, *J. Phys. B*, **3**, 1677-1691 (1970).
22. D. H. LEVY AND J. HINZE, *Astrophys. J.* **200**, 236-238 (1975).
23. H. M. MCCONNELL, *J. Chem. Phys.* **24**, 632-633 (1956).
24. G. VINCOW AND G. K. FRAENKEL, *J. Chem. Phys.* **34**, 1333-1343 (1961).
25. A. CARRINGTON AND A. D. MCLACHLAN, "Introduction to Magnetic Resonance," p. 138, Harper & Row, New York, 1967.
26. H. E. RADFORD, *Phys. Rev.* **126**, 1035-1045 (1962).
27. J. M. BROWN AND H. UEHARA, *Mol. Phys.* **24**, 1169-1174 (1972).
28. R. F. CURL, *Mol. Phys.* **9**, 585-597 (1965).